SLAC – PUB – 4064
August 1986
(I)

RECENT PROGRESS IN ČERENKOV RING IMAGING FOR THE SLD EXPERIMENT*

V. ASHFORD, T. BIENZ, F. BIRD, M. GAILLARD, G. HALLEWELL, D. LEITH, D. MCSHURLEY, A. NUTTALL, G. OXOBY, B. RATCLIFF, R. REIF, D. SCHULTZ, R. SHAW, S. SHAPIRO, T. SHIMOMURA,† E. SOLODOV,‡ N. TOGE,‖ J. VA'VRA, S. WILLIAMS§
Stanford Linear Accelerator Center, Stanford University, Stanford, CA 94305

D. BAUER, D. CALDWELL, A. LU, S. YELLIN
University of California, Department of Physics, Santa Barbara, CA 93106.

M. CAVALLI-SFORZA, P. COYLE, D. COYNE
Santa Cruz Institute for Particle Physics, University of California, Santa Cruz, CA 95064

R. JOHNSON, B. MEADOWS, M. NUSSBAUM
University of Cincinnati, Department of Physics, Cincinnati, OH 45221

Results of recent beam tests of a physics prototype Čerenkov Ring Imaging Detector (CRID) for the SLD experiment at the SLAC Linear Collider (SLC) are presented. The system includes both liquid (C_6F_{14}) and gas (isobutane) radiators and an 80 cm long Time Projection Chamber (TPC) with a gaseous TMAE (Tetrakis-Dimethylamino-Ethylene) photocathode and charge division readout of proportional wires. Handling of TMAE and development of a gas delivery system are discussed. Design considerations for the construction of the TPC anode planes are presented. Measurements of the multiplicity of detected Čerenkov photons, of Čerenkov angles, and the resolution with both radiators are presented. The particle identification capability of this detector is discussed.

1. INTRODUCTION

We describe the ongoing research and development[1] for the Čerenkov Ring Imaging Detector (CRID)[2–8] for the SLD experiment at the SLAC Linear Collider (SLC) (see Fig. 1).[4] The excellent particle identification provided by the CRID should allow the experiment to study the production and decay of Z^0 particles in great detail.

In the CRID designed for the SLD, ultraviolet Čerenkov radiation will be focused onto a 29 m^2 focal surface (Fig. 2) of quartz window TPCs. The photons are converted to photoelectrons in the TPC gas mixture of methane with either ethane or isobutane, together with the photoionising vapor TMAE ($E_i = 5.34$ eV). The combined use of liquid and gas radiators will afford good hadron identification over a wide momentum range up to 30 GeV/c and aid in π/e separation below 8 GeV/c.

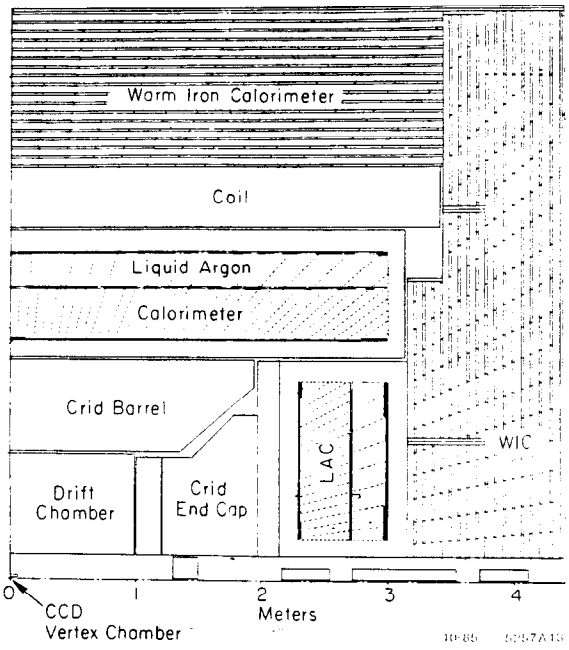

Fig. 1. Quadrant cross section of the SLD.

* Work supported in part by the Department of Energy, contract DE-AC03-76SF00515.
† Present Address: 2-80 Miya-Cho, Omiya, Saitama, Japan.
‡ Permanent Address: Institute of Nuclear Physics, Novosibirsk 630090, USSR.
‖ Speaker.
§ Present Address: Diasonics Corp., 533 Cabot St., S. San Francisco, CA 94080.

Presented at the XXIII International Conference on High Energy Physics, Berkeley, California, July 16-23, 1986

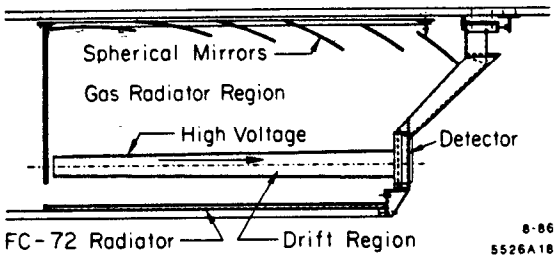

Fig. 2. Quadrant cross section of the SLD CRID.

Photoelectrons are drifted up to 1.2 m in the TPCs, and are detected by proportional wire chambers. The anode plane of a chamber is equipped with a charge-division readout to measure the depth coordinate of photoconversion points with a resolution of ~ 2 mm.[5]

In this paper we report results obtained with a prototype CRID module. Section 2 describes the apparatus, including the gas system which handles TMAE, and the proportional wire chamber. In Section 3 we present the beam test results, and discuss the particle identification capability of this detector. Section 4 gives conclusions.

2. APPARATUS

2.1 Design Principle

The equipment used in these studies is a test cell incorporating gas and liquid radiators (Fig. 3). The whole apparatus corresponds to about a half of one segment of the CRID system at SLD.[6]

A steerable U.V. coated spherical mirror (focal length = 50 cm) images the ring developed in the isobutane gas radiator (refractive index $\simeq$ 1.0016) to a desired position on one side of the TPC. Light from a 1.27 cm thick perfluorohexane (C_6F_{14}, refractive index $\simeq$ 1.277) liquid radiator is proximity-focused onto the opposite window of the TPC, producing a partial ring image. The size of the TPC is 4.5 cm in thickness, 20 cm in width and 80 cm in length (drift direction). Measurement of the conversion depth of each Čerenkov photon reduces the parallax broadening of ring images.

2.2 TMAE as a Gaseous Photocathode

The low ionization potential of TMAE allows the use of U.V. quartz windows, making construction of the CRID economically feasible. However, in the presence of parts per million (ppm) of protonic activators (*e.g.* water) TMAE readily reacts with oxygen. The oxidation products degrade the

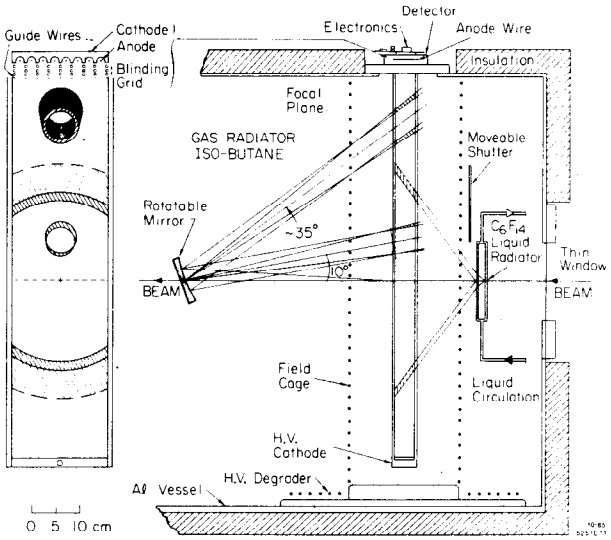

Fig. 3. Transverse view and elevation view of the prototype TPC. Trajectories of photons produced in the liquid and gas radiators are superimposed showing the expected images in the transverse view.

U.V. transmission and electron drift capabilities of the TPC gas which includes TMAE. Similar effects are produced by reactions with common "soft" sealing materials, such as neoprene, silicone rubber, *etc.* A carefully designed gas system and TMAE handling procedure are necessary.

Commercial TMAE contains about 3% impurities, 99% of which consist of the following components: Dimethylamine (DMA), Tetramethylhydrazine (TMH), Bis(dimethylamino)methane (BMAM), Dimethylformamide (DMF), Tetramethylurea (TMU), and Tetramethyloxamide (TMO). Of these, DMA is a strong absorber of U.V. photons, while TMO and TMU have high electron capture cross sections relative to oxygen. Removal of these impurities is essential for our experiment. To this end we have adopted the techniques developed by Holroyd *et al.*:[7] TMAE is (1) washed in deionized water, then (2) dried on molecular sieves, (3) filtered through silica gel, and (4) vacuum distilled. Samples of TMAE after each successive step have been analyzed with Gas Chromatography (GC) and Gas Chromatography/Mass Spectroscopy (GC/MS) techniques to measure the concentration of impurities.[8] The first two steps reduce impurities to less than 0.4%, and appear to be adequate for CRID work. TMAE processed through steps (1) and (2) has been used in subsequent studies.

The gas delivery system developed for this experiment was built with stainless steel components. No "soft" materials are exposed to TMAE liquid or vapor. The carrier gas (methane and ethane) is purified by molecular and Oxisorb filters,[10] reducing H_2O and O_2 contaminations to less than 1 ppm, and bubbled through liquid TMAE (processed as above) at a typical temperature of 28°C. The resulting TMAE partial pressure is 0.6 torr. The signals of drift electrons in this gas are measured at a variety of drift times. The attenuation time ("lifetime") of electrons during the drift is in the range from 50 to 100 μs. This is comparable with the electron lifetime in the gas without TMAE, and is acceptable for the maximum drift time (length) of 25 μs (1.2 m), expected at the SLD.

2.3 Proportional Chamber

The TPC proportional chamber is designed to maximize the detection efficiency for single photoelectrons. In addition, it has to keep the amount of "photon feedback" at a manageable level, and provide hit coordinate measurement along the anode wire. "Photon feedback" refers to the phenomenon where U.V. photons produced in the avalanche at an anode wire escape into the TPC fiducial volume, and ionize further TMAE molecules, producing secondary electrons which give rise to a noise background.

Photon feedback is suppressed with the chamber geometry shown in Fig. 4. The walls of the scallop-shaped cathode (nickel plated aluminum block) prohibit "direct communication" between neighboring anodes. Above the cathode are placed three layers of thick (0.9 mm diameter) wires topped by a layer of thin focusing wires (76 μ diameter). Electric potentials are applied to the wire arrays to efficiently focus drift electrons onto the anode, as shown in Fig. 4. The addition of this blinding grid reduces the number of feedback photons by a factor of 4. We observe less than 0.08 feedback photoelectrons per Čerenkov photoelectron.

The coordinate of U.V. photon conversion point along the anode wire is obtained by charge division readout of the wire signals. The anode plane is strung with 7 μ diameter carbon filaments[12] with a resistivity of 1600 $\mu\Omega$-cm. The anode wire length is 6 cm, corresponding to a typical total resistance of 25 kΩ. The wire spacing is 3.175 mm. Both ends of each filament are read out into a low noise preamplifier (LeCroy HQV810)

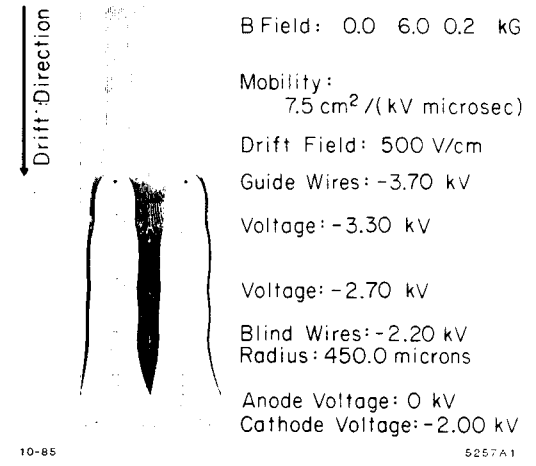

Fig. 4. Wire configuration of the chamber in the vicinity of anode wires. Electron drift paths are shown.

followed by a second HQV810 shaping stage, giving an overall rms noise charge of $\sim$ 1500 e. The use of carbon filaments as anode wires is important in gaining a good S/N ratio in the charge division analysis, since the thermal noise is inversely proportional to the square root of the anode resistivity. A cathode potential of -1.7 kV yields a gas gain of $\simeq 2 \times 10^5$ in the proportional mode of operation.

The amplified signals are read into 25 MHz CAMAC waveform samplers (LeCroy model 2241 Image Chamber Analyzers) which provide the drift coordinate (time) information for each photoelectron. Twenty wires are instrumented with readout electronics in the test described here, corresponding to a coverage of 6.35 cm in the wire address coordinate.

3. RESULTS FROM A BEAM TEST

In February 1986, data were taken with the prototype detector containing a drift gas mixture of 80% methane/20% ethane. The TMAE bubbler was operated at 28°C. A uniform electric field (400 V/cm) was generated in the TPC to drift photoelectrons at a typical drift velocity of 5 cm/μs.

Figure 5(a) shows an accumulation of 1500 gas radiator Čerenkov rings taken in an 11 GeV/c pion beam. The focusing mirror was tilted by 12.5° to shift the ring image from the particle impact point by $\simeq$ 20 cm. Displayed in Fig. 5(a) is the ring image projected onto the mirror focal plane. In this case all Čerenkov photons are assumed to have been converted at the mid-plane of the TPC, *i.e.* no charge division information is used.

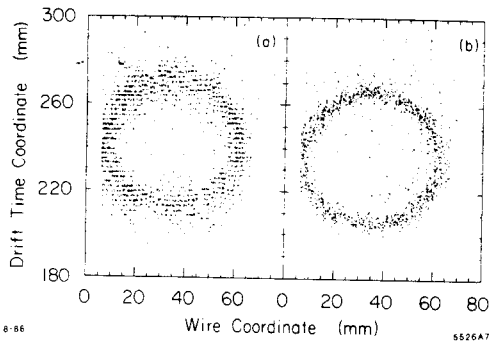

Fig. 5. (a) Gas radiator Čerenkov ring images for multiple events with parallax unresolved, and (b) with parallax corrected with charge division depth coordinate information. Units in x and y axes are mm.

Figure 6 shows the result of the charge division readout. The number of photo-electron signals is plotted against the charge asymmetry A,

$$A = \frac{Q_L - Q_R}{Q_L + Q_R}, \qquad (1)$$

where Q_L and Q_R denote the amount of charges collected on the two ends of anode wires. The value of A gives a measure of the depth coordinate of a photon conversion point. The slope of the distribution indicates a TMAE U.V. absorption length of 20.5 mm. This is consistent with an independent measurement made with a U.V. monochromator.

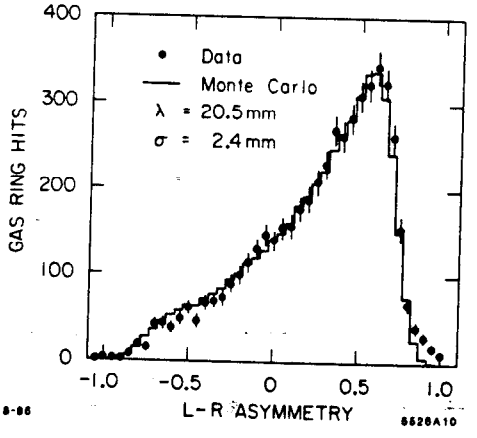

Fig. 6. Distribution of "charge asymmetry" defined by $(Q_L - Q_R)/(Q_L + Q_R)$ for gas ring signals. The asymmetry indicates the direction of the entry of the Čerenkov photons into the TPC.

Figure 5(b) shows the reduction of parallax error when the depth coordinate information is used. The hit radius of individual photons is shown in Fig. 7 for a sample of 650 events. The average measured point error of 2.09 ± 0.04 mm is in good agreement with the estimated overall error of $\sim$ 2 mm due to optical aberrations and the effects of diffusion and resolution in the TPCs. Use of the parallax correction in this case improves the gas ring image resolution by a factor of 2. From the average ring radius of 27.3 mm, we calculate the index of refraction of the radiator gas to be 1.00157 ± 0.00008.

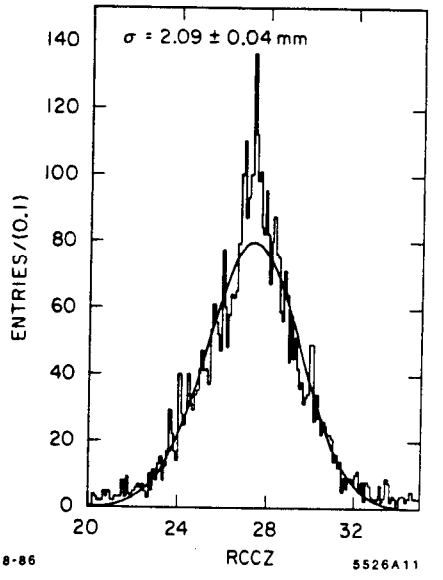

Fig. 7. Radius distribution (unit = mm) for parallax-corrected gas ring photons, with a Gaussian fit superimposed.

Figure 8 shows the distribution of the number of detected photoelectrons per gas ring; consistent with a Poisson mean of 8.6. Correcting for known losses due to photoconversion depth and electron lifetime, we expect 11.1 electrons per ring in the full detector, with a corresponding quality factor N_0,[18] of 85 cm^{-1}.

Figures 9(a) and (b) show typical gas rings for single π and K tracks at 11 GeV/c. The average radius of kaon ring image at 11 GeV/c is measured to be 16.6 ± 0.1 mm, while 16.4 mm is expected from the index of refraction 1.00157. The average number of photons observed per kaon ring is $3.33 \pm$ 0.3 (3.1 is expected), where the error is statistical only.

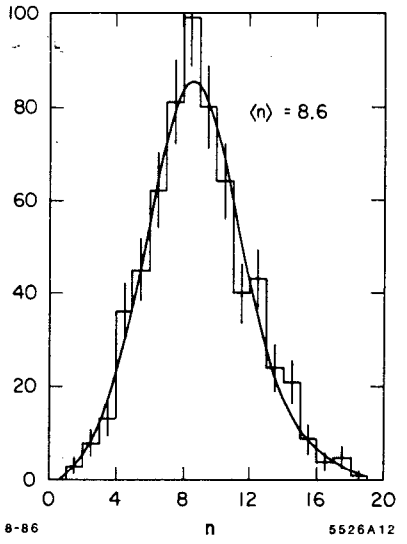

Fig. 8. Distribution of the number of observed photoelectrons per ring fitted to a Poisson distribution of $\langle n \rangle = 8.6$.

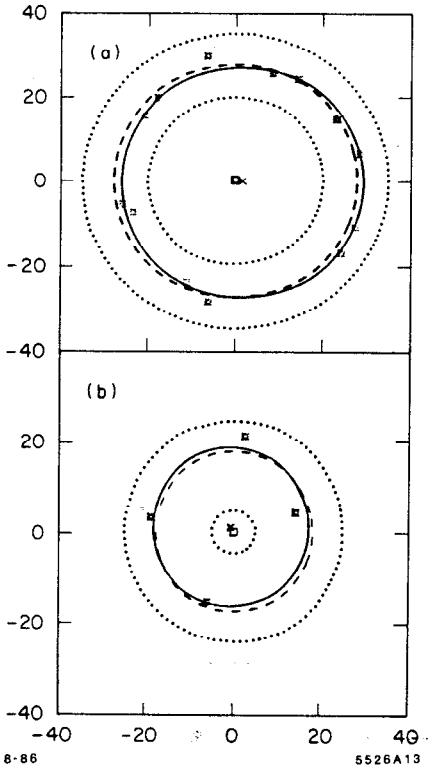

Fig. 9. (a) Gas ring for a single 11 GeV/c pion track, and (b) for a single 11 GeV/c kaon track. The star symbols show the observed photoconversion points. Units of the x and y axes are mm.

In Figures 10(a) and (b) we illustrate improvement in the Čerenkov angle measurement of the signals from the liquid radiator obtained with the use of depth coordinate information. The resolution obtained for single photoelectrons is $\sigma = 0.91°$ around a nominal photon angle of $\sim 52°$ after refraction, compared to an expectation of 0.86°. The mean number of observed photoelectrons on the incomplete liquid ring leads us to expect 34 on the full ring after corrections for the loss due to the finite electron drift "lifetime". This corresponds to an N_0 of 86 cm^{-1}.

The particle separation expected with gas and liquid radiators is shown in Figures 11(a) and (b). The 1σ bands are indicated for particle species, e, π, K and protons.

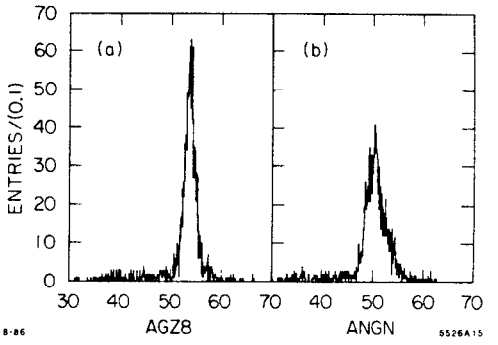

Fig. 10. (a) Liquid radiator ring Čerenkov angle, corrected for parallax, and (b) uncorrected for parallax. Units are degrees.

4. CONCLUSIONS

We have built and tested a prototype module of the Čerenkov Ring Imaging Detector, and demonstrated its feasibility. We have developed a TMAE handling procedure and constructed a reliable gas delivery system. An effective method for reducing the photon feedback on the proportional wires has been developed and tested. Charge division readout of the anode signals has provided satisfactory resolution for determination of the photon conversion points. This performance, transformed to the SLD experiment, will provide very powerful particle identification capability over a wide momentum range.

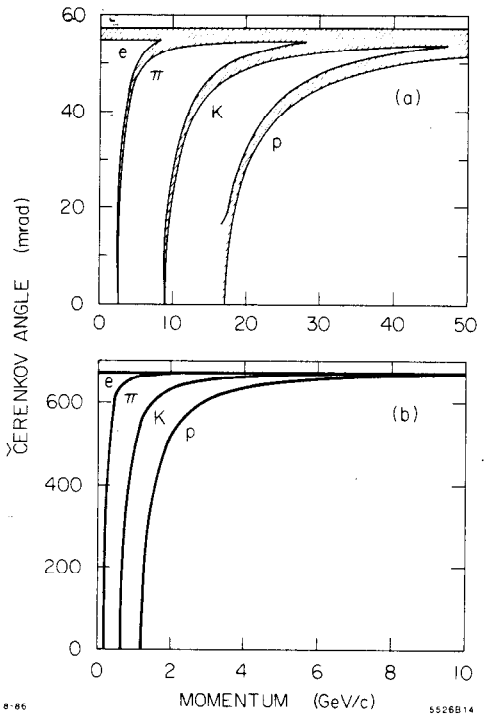

Fig. 11. Estimated particle separation as function of momentum with (a) the gas radiator and with (b) the liquid radiator. Indicated are 1σ separation bands expected at the SLD, based on the prototype results.

REFERENCES

1. Much work in this field has been performed by the DELPHI-RICH group at CERN. Their latest results are reported in R. Arnold et al., LPC 86/09, Invited Talk at Vienna Conf. on Wire Chambers, Vienna (1986), and references therein.
2. S. Williams et al., IEEE Trans. Nucl. Sci., NS32, 681 (1985). Also, see S. Williams, "Čerenkov Ring Imaging Detector Development at SLAC," SLAC-PUB-3360 (1984).
3. V. Ashford et al., IEEE Trans. Nucl. Sci., NS33, 113 (1986).
4. M. Breidenbach, IEEE Trans. Nucl. Sci., NS33, 46 (1986).
5. F. Bird et al., IEEE Trans. Nucl. Sci., NS33, 261 (1986).
6. The barrel part of the SLD CRID in the current design is azimuthally segmented into 20 drift sections.
7. R.A. Holroyd, S. Ehrenson and J.M. Preses, Jour. Phys. Chem. 89, 424 (1985).
8. R.T. Rewick, et al. in preparation.
9. Manufactured by Messer Greisheim Co., West Germany.
10. Carbon filaments manufactured by American Cyanamid Inc, with 7 micron diameter, breaking strength 450,000 psi.
11. N_0 is an efficiency parameter (cm^{-1}) which relates the observed number of photoelectrons N_{pe}, radiator thickness L and Čerenkov angle θ_c as: $N_{pe} = N_0 L \sin^2\theta_c$.